

## UNIAXIAL PML ABSORBING BOUNDARY CONDITION FOR TRUNCATING THE BOUNDARY OF DNG META-MATERIALS

**K. S. Zheng**

School of Electronics and Information  
Northwestern Polytechnical University  
Chang'an Campus, Xi'an 710072 Shaanxi, China

**W. Y. Tam**

Department of Electronic and Information Engineering  
The Hong Kong Polytechnic University  
Kowloon, Hong Kong, China

**D. B. Ge**

School of Science  
Xidian University  
Xi'an, Shaanxi 710071, China

**J. D. Xu**

School of Electronics and Information  
Northwestern Polytechnical University  
Chang'an Campus, Xi'an 710072 Shaanxi, China

**Abstract**—The conventional perfectly matched layer (PML) absorbing boundary condition is shown to be unstable when it is extended to truncate the boundary of the double negative (DNG) medium. It is a consequence of the reverse directions of the Poynting and phase-velocity vectors of plane waves propagating in such material. In this paper, a modified uniaxial PML (UPML), which is stable for the DNG medium, is derived. The auxiliary differential equation technique is introduced to derive the discrete field-update equations of DNG-UPML. Numerical results demonstrate the effectiveness and stability of the new UPML for the DNG medium.

---

Corresponding author: K. S. Zheng (kszheng@nwpu.edu.cn).

## 1. INTRODUCTION

The plane-wave propagation in a material whose permittivity and permeability are assumed to be simultaneously negative is theoretically investigated by Veselago [1]. Recently, several papers have exposed the usefulness of double negative (DNG) medium with negative permittivity and permeability [2–5]. However, in order to further study unusual electromagnetic phenomena in DNG medium, full-wave numerical simulations have become more and more important. The FDTD method is a good choice for these electromagnetic problems. The absorbing boundary condition in FDTD is required to truncate the computation domain without reflection in the simulation of DNG medium properties and applications. An absorbing boundary condition for DNG medium has been proposed [6, 7]. Since first introduced by Berenger in 1994 [8], the perfectly matched layer (PML) has become the most popular and efficient absorbing boundary condition. Unfortunately, standard versions of PML are inherently unstable when they are extended to truncate the boundary of DNG medium without any modification [9, 10]. Recently, a nearly PML absorbing boundary condition for DNG medium is discussed, and 50-cell layers for NIMPML are used to truncate the DNG medium [10]. Later, a modified PML absorbing boundary condition based on the complex-coordinate stretching variables has been proposed for PSTD method [11]. In this paper, a modified uniaxial PML (UPML) which is stable for the DNG medium is presented. It is worth noting that only 10-cell layers for UPML are used and provide a clearly reduced error to truncate the DNG medium.

First, we adopt the UPML medium for truncating the DNG medium. Then, by using the auxiliary differential equation technique, the efficient DNG-UPML is implemented in the FDTD method. Finally, the relative error of DNG-UPML in the one-dimensional case is calculated, and the focusing property of a DNG medium is also simulated. A numerical example was used to demonstrate the stability of the proposed DNG-UPML absorbing boundary condition.

## 2. NUMERICAL METHOD

### 2.1. Maxwell's Equations in the DNG Medium

The time-harmonic Maxwell's curl equations to be solved are:

$$j\omega\epsilon\mathbf{E} = \nabla \times \mathbf{H} \quad (1)$$

$$-j\omega\mu\mathbf{H} = \nabla \times \mathbf{E} \quad (2)$$

By replacing the derivatives with their central finite difference counterparts, the FDTD formulations of (1) and (2) can be obtained easily. For a lossy DNG material, negative permittivity and permeability are realized using the Drude medium model as follows:

$$\varepsilon(\omega) = \varepsilon_0 \varepsilon_r(\omega) = \varepsilon_0 \left( 1 + \frac{\omega_{pe}^2}{\omega(j\Gamma_e - \omega)} \right) \quad (3)$$

$$\mu(\omega) = \mu_0 \mu_r(\omega) = \mu_0 \left( 1 + \frac{\omega_{pm}^2}{\omega(j\Gamma_m - \omega)} \right) \quad (4)$$

### 2.2. UPML for the DNG Medium

For a matched condition, the permittivity and permeability in the UPML can be written as  $\varepsilon(\omega) = \varepsilon_0 \varepsilon_r(\omega) \bar{s}$  and  $\mu(\omega) = \mu_0 \mu_r(\omega) \bar{s}$ , where  $\bar{s}$  is the diagonal tensor defined by:

$$\bar{s} = \begin{bmatrix} s_y s_z s_x^{-1} & 0 & 0 \\ 0 & s_x s_z s_y^{-1} & 0 \\ 0 & 0 & s_x s_y s_z^{-1} \end{bmatrix} \quad (5)$$

In order to truncate the DNG medium, a good choice for  $s_i$  ( $i = x, y, z$ ) in (5) is:

$$s_i = \kappa_i + \frac{\sigma_i}{j\omega\varepsilon_0\sqrt{\mu_r\varepsilon_r}} = \kappa_i + \frac{\sigma_i}{j\omega\varepsilon_0 \left( 1 + \frac{\omega_p^2}{\omega(j\Gamma - \omega)} \right)} \quad (6)$$

where  $\omega_p = \omega_{pe} = \omega_{pm}$  and  $\Gamma = \Gamma_m = \Gamma_e$ .

From (1) to (6), the Ampere's law in a matched DNG-UPML can be expressed as

$$\begin{bmatrix} \frac{\partial H_z}{\partial y} - \frac{\partial H_y}{\partial z} \\ \frac{\partial H_x}{\partial z} - \frac{\partial H_z}{\partial x} \\ \frac{\partial H_y}{\partial x} - \frac{\partial H_x}{\partial y} \end{bmatrix} = j\omega\varepsilon_0\varepsilon_r(\omega) \begin{bmatrix} \frac{s_y s_z}{s_x} & 0 & 0 \\ 0 & \frac{s_x s_z}{s_y} & 0 \\ 0 & 0 & \frac{s_x s_y}{s_z} \end{bmatrix} \begin{bmatrix} E_x \\ E_y \\ E_z \end{bmatrix} \quad (7)$$

where the assumed tensor coefficients in  $x, y,$  and  $z$  directions for the

DNG medium are:

$$\begin{cases} s_x = \kappa_x + \frac{\sigma_x}{j\omega\varepsilon_0\sqrt{\mu_r\varepsilon_r}} \\ s_y = \kappa_y + \frac{\sigma_y}{j\omega\varepsilon_0\sqrt{\mu_r\varepsilon_r}} \\ s_z = \kappa_z + \frac{\sigma_z}{j\omega\varepsilon_0\sqrt{\mu_r\varepsilon_r}} \end{cases} \quad (8)$$

In order to derive the discrete field-update equations for (7), we adopt auxiliary differential equation FDTD techniques that permit direct time integration of the full-vector Maxwell's equations [12]. Now, substituting (8) into (7), the system of equations in (7) can be transformed into time domain and be discretized on the standard Yee lattice. This yields time-stepping expressions for  $E_x$ ,  $E_y$ , and  $E_z$ . For example, the  $E_x$  updating equation is given by:

$$\begin{aligned} E_x^{n+1} = & \frac{1}{\frac{b_1}{2\Delta t} + \frac{b_2}{\Delta t^2} + \frac{b_3}{4}} \left[ \left( \frac{2b_2}{\Delta t^2} - \frac{b_3}{2} \right) E_x^n + \left( \frac{b_1}{2\Delta t} + \frac{b_2}{\Delta t^2} + \frac{b_3}{4} \right) E_x^{n-1} \right. \\ & + \left( \frac{a_1}{2\Delta t} + \frac{a_2}{\Delta t^2} + \frac{a_3}{4} \right) R_x^{n+1} + \left( \frac{a_3}{2} - \frac{2a_2}{\Delta t^2} \right) R_x^n \\ & \left. + \left( \frac{a_2}{\Delta t^2} - \frac{a_1}{2\Delta t} + \frac{a_3}{4} \right) R_x^{n-1} \right] \end{aligned} \quad (9)$$

where the parameters are:

$$\begin{cases} a_1 = \sigma_x + \kappa_x\Gamma, & a_2 = \kappa_x, & a_3 = \sigma_x\Gamma + \kappa_x\omega_p^2 \\ b_1 = \sigma_y + \kappa_y\Gamma, & b_2 = \kappa_y, & b_3 = \sigma_y\Gamma + \kappa_y\omega_p^2 \end{cases} \quad (10)$$

The auxiliary field variable  $R_x$  can be updated using:

$$\begin{aligned} R_x^{n+1} = & \left( \frac{2\varepsilon_0\kappa_z - \varepsilon_0\sigma_z\Delta t - \beta_d\Delta t}{2\varepsilon_0\kappa_z + \varepsilon_0\sigma_z\Delta t + \beta_d\Delta t} \right) R_x^n \\ & + \frac{2\Delta t}{2\varepsilon_0\kappa_z + \varepsilon_0\sigma_z\Delta t + \beta_d\Delta t} \left[ (\nabla \times H)|_x^n - \frac{1}{2}(k_d + 1)J_x^n \right] \end{aligned} \quad (11)$$

where the expression of  $(\nabla \times H)|_x^n$  denotes the  $x$ -directed curl of magnetic field quantity calculated at the time point  $t_n = n\Delta t$ . The updating equation of the variable  $J_x$  can be written as:

$$J_x^{n+1} = k_d J_x^n + \beta_d (R_x^{n+1} + R_x^n) \quad (12)$$

where the parameters  $k_d$  and  $\beta_d$  are defined as:

$$\begin{cases} k_d = \frac{2 - \Gamma \Delta t}{2 + \Gamma \Delta t} \\ \beta_d = \frac{\varepsilon_0 \omega_p^2 \kappa_z \Delta t}{2 + \Gamma \Delta t} (R_x^{n+1} + R_x^n) \end{cases} \quad (13)$$

Similar expressions can be derived for the remaining two  $E$ -field components in the lossy DNG-UPML. Overall, updating the components of  $E$  in the DNG-UPML requires three steps. First, obtaining the new values of the components of  $J$  according to (12); second, using these new  $J$  components to obtain the new values of the components of  $R$  according to (11); and third, using these new  $R$  components to obtain the new values of the  $E$  components according to (9).

A similar three-step procedure can be derived to update the components of  $H$  in the DNG-UPML using the same approach.

### 3. NUMERICAL RESULTS

In this section, numerical results are presented in both one-dimensional and two-dimensional cases. The relative error of DNG-UPML absorbing boundary condition in one-dimensional case is also discussed.

#### 3.1. One-dimensional Case

The time function of line electric-current source is given by the multiple cycle  $m$ - $n$ - $m$  pulse [13]. It is a sinusoidal signal that has a smooth windowed turn-on for  $m$  cycles, constant amplitude for  $n$  cycles, and then a smooth windowed turn-off for  $m$  cycles. Hence, it has an adjustable bandwidth centered at the frequency  $f_0$ , as shown in Fig. 1.

First, we show the performance of the DNG-UPML. The one-dimensional structure under study is shown in Fig. 2. The total space of the computational domain is filled with the DNG medium, where the parameters in (3) and (4) are as follows:  $\Gamma_e = \Gamma_m = \Gamma = 0$  and  $\omega_{pe} = \omega_{pm} = \omega_p = 2.665 \times 10^{11}$  rad/s. The UPML ABC is used to truncate the boundary of DNG medium. An  $x$ -directed electric line current source is located at the center of a 4000-cell one dimensional FDTD grid. The center frequency  $f_0$  of the current source is 30 GHz, and its time function is the 5-10-5 pulse. In particular, the values of  $\text{Re}(\varepsilon_r)$  and  $\text{Re}(\mu_r)$  at the center frequency  $f_0$  are approximately  $-1.0$ .

The FDTD grid has  $\Delta z = 0.01$  cm and a time-step of 0.5 times the Courant limit. The  $E$ -field is probed at point A, as shown in Fig. 2. Point A is one cell from the right-side PML boundary. Time-stepping

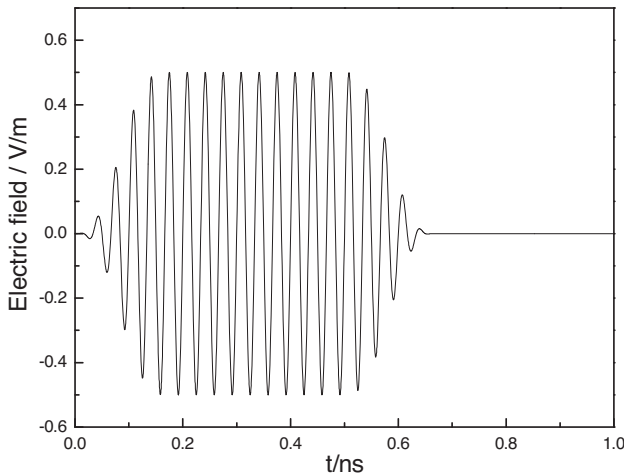


**Figure 1.** Waveform of the electric current source in time domain.

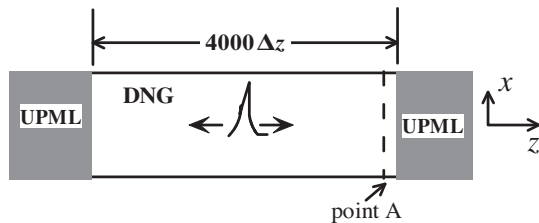


**Figure 2.** Sketch of numerical simulation.

runs over 22,000 iterations, well past the steady-state response. 10-cell UPML ABCs are used with a cubic polynomial increase of  $\sigma$  with distance and with  $\sigma_{\max} = \sigma_{opt}$  [14], and  $\kappa_{\max} = 1$ , yielding the properties of UPML.

The reference solution  $E_{\text{ref}}|_k^n$  at grid location  $k$  and time-step  $n$  is obtained using a 40,000-cell grid. An identical current source is centered within this grid, and the field-observation point A is at the same position relative to the source as in the test grid. The reference grid is large enough such that there are no reflections from its outer boundaries during the time-stepping span of interest. This allows a relative error to be defined as:

$$R_{\text{error}}|_k^n = 20 \log_{10} \left( |E|_k^n - E_{\text{ref}}|_k^n \right) / |E_{\text{ref max}}|_k \quad (14)$$

where  $E_{\text{ref max}}|_k$  is the maximum amplitude of the reference field at the location  $k$ , as observed during the time-stepping span of interest.

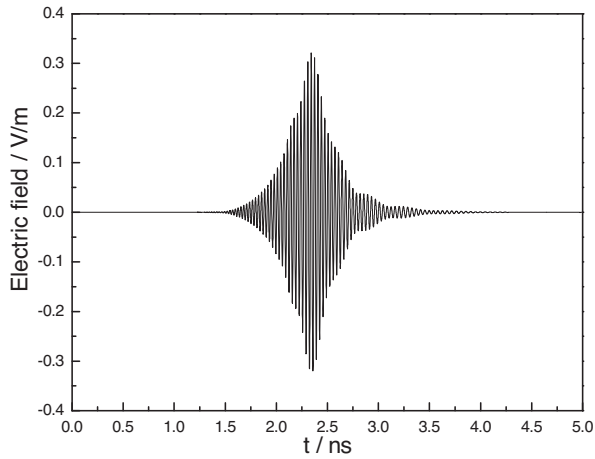


**Figure 3.** Stable time-domain field for DNG-UPML.

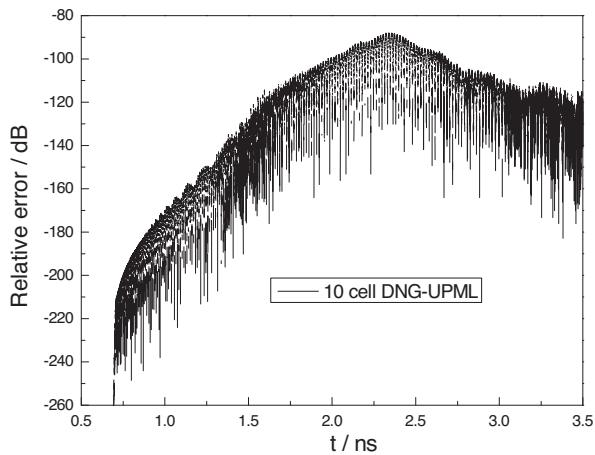


**Figure 4.** Relative error at point A for 10-cell PMLs.

Fig. 3 shows the DNG-UPML simulation is stable enough to compute a solution for at least 100,000 time steps, which is equal to 16.7 ns in the absolute time domain. Fig. 4 depicts the relative error at point A over 22,000 time-steps of the FDTD run for 10-cell PMLs. From Fig. 4, we see that the DNG-UPML absorbing boundary condition achieves a very small reflection at the boundary. The maximum relative error is below 80 dB. This accuracy is good enough to simulate a lot of numerical simulations of the electromagnetic problems in DNG medium.

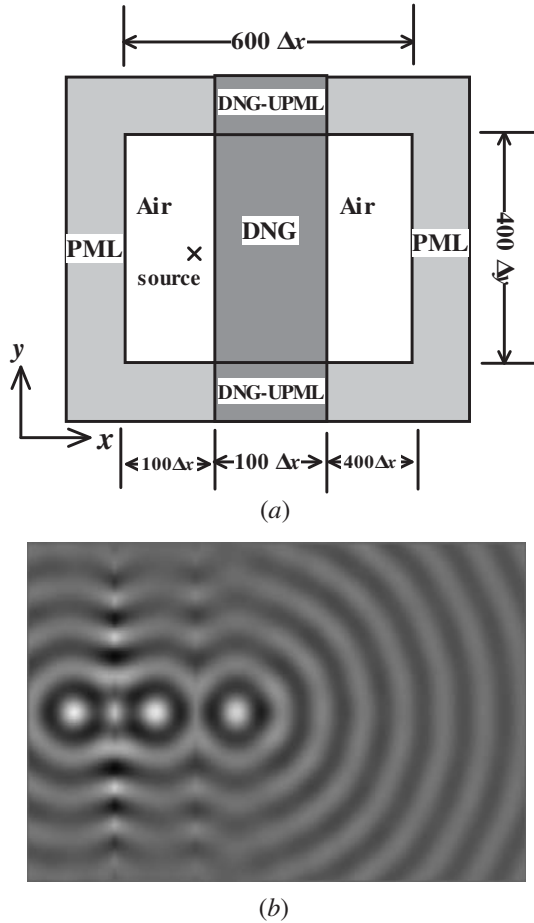


**Figure 5.** Simulation of the focus property of DNG medium. (a) The geometry of the computation domain. (b) Snapshot taken at  $t = 5925\Delta t$ .

### 3.2. Two-dimensional Case

In this section, we consider the perfect lens focusing property of DNG medium. A two-dimensional TM wave is considered. The frequency of the harmonic line current source is set to 30 GHz. The two dimensional geometry under study is shown in Fig. 5(a), and the sizes of the geometry and the computation domain are also indicated. The cell sizes are  $\Delta x = \Delta y = 0.02$  cm. The time step is set to be  $\Delta t = \Delta x/(2c)$ . The FDTD grid is terminated with standard PML and DNG-UPML



derived above. Both are ten cells long with a 4-power polynomial increase of  $\sigma$  with distance and with  $\sigma_{\max} = \sigma_{opt}$ , and  $\kappa_{\max} = 1$ . In order to view the perfect lens foci, the parameters of the lossless DNG slab are similar to that in the one-dimensional case. The slab is thus  $d = 100\Delta x$  thick in the direction of propagation and the source-to-slab distance is  $50\Delta x$ . A snapshot of the electric field intensity  $E_z$  over the whole computation domain is taken at  $t = 5925\Delta t$ , as shown in Fig. 5(b). The foci inside and outside the DNG slab can be seen clearly because of the effect of negative refraction in the DNG medium. It is worth noting that the DNG-UPML simulation applied to truncating the DNG medium is also stable in the two-dimensional case.

#### 4. CONCLUSION

In this paper, a new DNG-UPML absorbing boundary condition has been derived in order to overcome the instability of standard PML for truncating the boundary of the DNG medium. Using the auxiliary differential equation approach, the efficient formulations of the DNG-UPML are presented. Numerical FDTD simulations of these one-dimensional and two-dimensional cases are provided. Numerical results have demonstrated the accuracy and stability of the DNG-UPML absorbing boundary condition.

#### ACKNOWLEDGMENT

This work was supported in part by the Research Grants Council of the Hong Kong Administrative Region, China, under Grant PolyU 5262/05E.

#### REFERENCES

1. Veselago, V. G., "The electrodynamics of substances with simultaneously negative values of  $\epsilon$  and  $\mu$ ," *Sov. Phys. Usp.*, Vol. 10, No. 4, 509–514, 1968.
2. Shelby, R. A., D. R. Smith, S. C. Nemat-Nasser, and S. Schultz, "Microwave transmission through a two-dimensional, isotropic, left-handed metamaterial," *Appl. Phys. Lett.*, Vol. 78, 489–491, 2001.
3. Shelby, R. A., D. R. Smith, and S. Schultz, "Experimental verification of a negative index of refraction," *Science*, Vol. 292, 77–79, 2001.

4. Smith, D. R. and N. Kroll, "Negative refractive index in left-handed materials," *Phys. Rev. Lett.*, Vol. 85, 2933–2936, 2000.
5. Pendry, J. B., "Negative refraction makes a perfect lens," *Physical Review Letter*, Vol. 85, 3966–3969, 2000.
6. Wittwer, D. C. and R. W. Ziolkowski, "Two time-derivative Lorentz material (2TDLM) formulation of a Maxwellian absorbing layer matched to a lossy media," *IEEE Trans. Antennas Propag.*, Vol. 48, No. 2, 192–199, 2000.
7. Wittwer, D. C. and R. W. Ziolkowski, "Maxwellian material based absorbing boundary conditions for lossy media in 3D," *IEEE Trans. Antennas Propag.*, Vol. 48, 200–213, 2000.
8. Berenger, J. P., "A perfectly matched layer for the absorbing EM waves," *J. Computat. Phys.*, Vol. 114, 185–200, 1994.
9. Dong, X. T., X. S. Rao, Y. B. Gan, B. Guo, and W. Y. Yin, "Perfectly matched layer-absorbing boundary condition for left-handed materials," *IEEE Microwave Wireless Compon. Lett.*, Vol. 14, 301–303, 2004.
10. Cummer, S. A., "Perfectly matched layer behavior in negative refractive index materials," *IEEE Antennas Wireless Propagat. Lett.*, Vol. 3, 172–175, 2004.
11. Shi, Y., Y. Li, and C. H. Liang, "Perfectly matched layer absorbing boundary condition for truncating the boundary of the left-handed medium," *Microwave Opt. Technol. Lett.*, Vol. 48, No. 1, 57–62, 2006.
12. Taflove, A. and S. C. Hagness, *Computational Electrodynamics: The finite-difference time-domain method*, 3rd edition, Artech House, Norwood, MA, 2005.
13. Ziolkowski, R. W. and A. D. Kipple, "Causality and double-negative metamaterials," *Physical Review E*, Vol. 68, 026615, 2003.
14. Gedney, S. D., "An anisotropic perfectly matched layer absorbing media for the truncation of FDTD lattices," *IEEE Trans. Antennas Propagat.*, Vol. 44, 1630–1639, 1996.